Chemical Engineering Journal 156 (2010) 70–76

Contents lists available at ScienceDirect

Chemical Engineering Journal

journal homepage: www.elsevier.com/locate/cej

Structural effects on the interactions of benzene and naphthalene sulfonates with activated carbon cloth during adsorption from aqueous solutions

Erol Ayranci[a,*], Osman Duman[b]

[a] Chemistry Department, Faculty of Arts and Sciences, Akdeniz University, Dumlupinar Boulvard, 07058 Antalya, Turkey
[b] Faculty of Education, Akdeniz University, 07058 Antalya, Turkey

ARTICLE INFO

Article history:
Received 2 April 2009
Received in revised form
18 September 2009
Accepted 21 September 2009

Keywords:
Adsorption kinetics
Adsorption isotherm
Activated carbon cloth
Benzene sulfonates
Naphthalene sulfonates
In-situ UV spectroscopy

ABSTRACT

Interactions of benzene and naphthalene sulfonates with activated carbon cloth (ACC) during adsorption from aqueous solutions were investigated. Systematically chosen sulfonates were sodium salt of benzene sulfonic acid (NaBS), disodium salt of 1,3-benzene disulfonic acid (Na_2BDS), sodium salt of 1-naphthalene sulfonic acid (NaNS), disodium salt of 1,5-naphthalene disulfonic acid (Na_2NDS) and trisodium salt of 1,3,(6 or 7)-naphthalene trisulfonic acid (Na_3NTS). The adsorption behaviors of these adsorbates from solutions in water and in 0.01 M H_2SO_4 onto the ACC were monitored by in-situ UV–visible spectroscopic technique. The order of rates and extents of adsorption of sulfonates were explained in terms of acidity of the medium and structural factors influencing the interactions between sulfonates and the ACC surface. Kinetic data of adsorption were treated according to pseudo first-order, pseudo second-order, Elovich and intra-particle diffusion models. The best model representing the experimental kinetic data was found to be the pseudo second-order model. Adsorption isotherms of the sulfonates onto the ACC were derived at 30 °C. Isotherm data were found to fit the Freundlich model better than the Langmuir model.

1. Introduction

Benzene and naphthalene sulfonates are used widely in several industries. Naphthalene sulfonates and their derivatives have been applied in the paper, textile and tanning industries as optical brighteners, dispersants and wetting agents. Benzene sulfonates are used in the production of dyestuffs, tanning agents, catalysts, pesticides, ion exchange resins, optical brighteners, wetting and finishing agents, plasticizers, pharmaceuticals and chemicals for organic synthesis [1,2]. Benzene and naphthalene sulfonates are highly soluble in water. As they are highly toxic and are only slowly biodegradable [3], benzene and naphthalene sulfonates must be removed or destructed from waste-waters of the above mentioned industries.

The removal studies mostly involve adsorption of pollutants onto suitable adsorbents. Activated carbon is one of the most widely used adsorbents for the adsorption of organic compounds. There are three types of activated carbon; powder activated carbon, granular activated carbon and activated carbon cloth (ACC). Recently, ACC has received considerable attention as a potential adsorbent for water treatment applications. Activated carbon cloth or fiber has several unique characteristics compared with conventionally used granular or powder activated carbons. These materials are composed of thin fibers of the order of 10 μm in diameters leading to greater adsorption rates, and hence contributing to the minimization of the reactor size. The cloth or fiber form of activated carbon also makes the handling of adsorbents much easier [4,5].

The adsorption capacity of an activated carbon depends on: (i) the nature of the adsorbent (e.g. surface functional groups, specific surface area and pore size distribution); (ii) the nature of adsorbate (e.g. functional groups, polarity, hydrophobicity, size, solubility and pK_a or pK_b for weak acids or bases); and (iii) conditions of adsorption medium (e.g. pH, temperature, adsorbate concentration and polarity of solvent) [6].

There is not much study on the removal of benzene and naphthalene sulfonates from water reported in the literature. Sheindorf et al. [7] studied the adsorption of benzene sulfonate, parabromophenol and phenol onto the granular activated carbon at 25 °C. The adsorption of 1,3,6-naphthalenetrisulfonic acid on a commercial activated carbon (Filtrasorb 400) in the presence of Cd(II), Cr(III) and Hg(II) was investigated by Rivera-Utrilla et al. [8]. They found that the adsorption capacity of 1,3,6-naphthalenetrisulfonic acid on activated carbon increased in the presence of Cd(II) and Cr(III), whereas the adsorption process was not affected by the presence of Hg(II). Esposito et al. [9] reported the sorption of naphthalene sulfonate compounds on soil. We have not met any study about the adsorption of benzene and naphthalene sulfonates onto the ACC reported in literature.

---

* Corresponding author. Tel.: +90 242 310 23 15; fax: +90 242 227 89 11.
E-mail addresses: eayranci@akdeniz.edu.tr (E. Ayranci), osmanduman@akdeniz.edu.tr (O. Duman).

1385-8947/$ – see front matter © 2009 Elsevier B.V. All rights reserved.
doi:10.1016/j.cej.2009.09.038

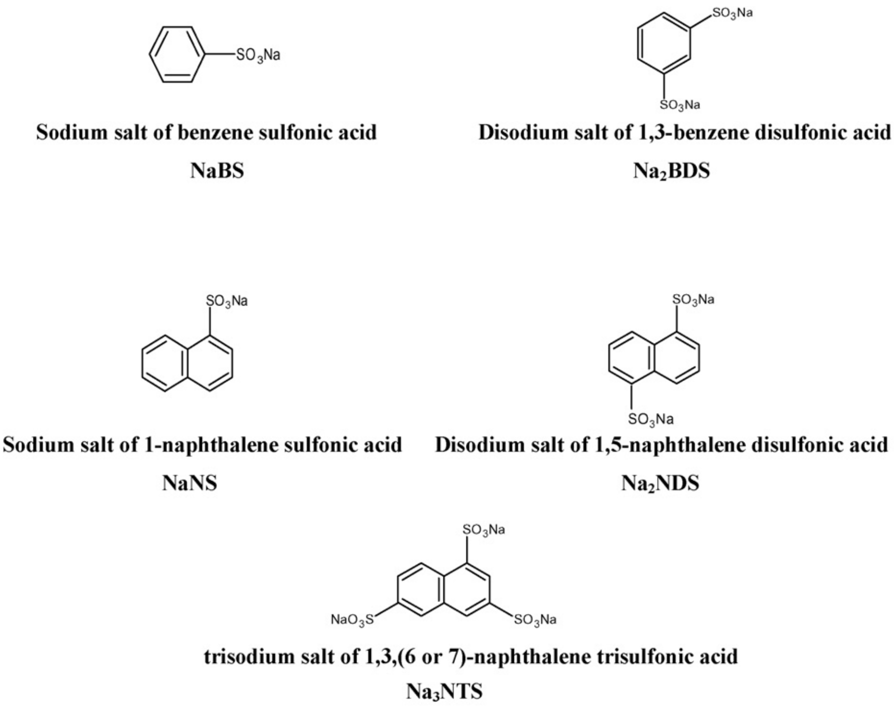

Fig. 1. Chemical structures of benzene and naphthalene sulfonates.

The aim of the present study is to investigate the adsorption behaviors of various sodium salts of benzene and naphthalene sulfonic acids onto the ACC by in-situ UV–visible spectroscopic method and also to examine the effects of pH and structural factors such as number of aromatic rings, number and position of sulfonate groups on the adsorption behaviors of sulfonates.

2. Materials and methods

2.1. Materials

The ACC used in the present work was obtained from Spectra Corp. (MA, USA) coded as Spectracarb 2225. Although the full details of its mode of preparation are regarded as proprietary, it originates from pyrolysis of phenolic polymer fibers followed by heat treatment in O_2-free N_2 between 800 and 900 °C for some hours. In this respect, it differs from other fibrous carbon materials derived by pyrolysis of rayon [10].

Sodium salt of benzene sulfonic acid (NaBS) with a purity of 95% and disodium salt of 1,5-naphthalene disulfonic acid (Na_2NDS) with a purity of 95% were obtained from Aldrich, disodium salt of 1,3-benzene disulfonic acid (Na_2BDS) with a purity of 95% and sodium salt of 1-naphthalene sulfonic acid (NaNS) with a purity of 99% from ABCR and trisodium salt of 1,3,(6 or 7)-naphthalene trisulfonic acid (Na_3NTS) with a purity of 80% from Fluka. The molecular structures of these benzene and naphthalene sulfonates are given in Fig. 1. Deionized water was used in adsorption experiments.

2.2. Treatment and properties of the ACC

A washing procedure was applied for the ACC as described previously [10–12]. Several properties of the ACC such as specific surface area, volumes of micropores and mesopores, elemental composition, pH_{PZC} which is the pH of solution at which net charge on the surface of the ACC is zero, and acidic and basic group contents were determined in our previous works [11–13]. These properties are listed in Table 1. The SEM pictures and electrochemical characterization of the ACC were also reported earlier [14].

2.3. The design of the adsorption cell and optical absorbance measurements

A specially designed cell was used to carry out the adsorption and simultaneously to perform in-situ concentration measurements by means of UV–visible absorption spectrophotometry. This cell, described in detail including a diagram in our previous works [11,12,15,16], was V-shaped with one arm containing the carbon cloth attached to a short Pt wire sealed to a glass rod and the other arm containing a thin glass tube through which N_2 gas was passed for the dual purposes of mixing and eliminating any dissolved CO_2. The two arms were connected to a glass joint leading to a vacuum pump at the upper part of the V-shaped cell in order to provide the opportunity for initial outgassing of the carbon adsorbent and the cell and solution. A quartz spectrophotometer cuvette was sealed to the bottom of the adsorption cell.

With the use of the adsorption cell described above it was possible to follow the changes in concentration of the adsorbate solution during the course of adsorption by in-situ UV–visible spectroscopy. Solutions of adsorbates were prepared in water or in 0.01 M H_2SO_4.

Table 1
Properties of the ACC.

Specific surface area	1870 $m^2\,g^{-1}$
Total pore volume	0.827 $cm^3\,g^{-1}$
Micropore volume	0.709 $cm^3\,g^{-1}$
Mesopore volume	0.082 $cm^3\,g^{-1}$
Average fiber diameter	17 μm
Carbon content	95.14%
Hydrogen content	0.37%
Oxygen content	4.49%
Nitrogen and sulfur content	0%
pH_{PZC}	7.4
Total acidic group content	0.25 $mmol\,g^{-1}$
Carboxylic group content	0.093 $mmol\,g^{-1}$
Lactonic group content	0.020 $mmol\,g^{-1}$
Phenolic group content	0.14 $mmol\,g^{-1}$
Total basic group content	0.28 $mmol\,g^{-1}$

The initial concentrations of benzene and naphthalene sulfonates and the amount of the ACC were kept as constant as possible for kinetic study of adsorption of each sulfonate in order to make an easy comparison among adsorption behaviors of different benzene and naphthalene sulfonates (concentration: 1×10^{-4} M, mass of the ACC: 18.3 ± 0.1 mg). The ACC pieces were pre-wetted by leaving in water for 24 h before use. During this long contact period with water, the pores of the ACC may expand and become more accessible for the adsorbates, in the actual adsorption process. The idea of using pre-wetted ACC originated from our previous findings that pre-wetting enhances the adsorption process [14,15].

The ACC piece was dipped into the adsorption cell initially containing only water and vacuum was applied to remove all air in the pores of the ACC. Then wetted and degassed ACC was removed from the cell, temporarily, for a short time and water in the cell was replaced with a known volume of sample solution (20 mL). The sliding door of the sample compartment of the spectrophotometer was left half-open and quartz cuvette fixed at the bottom of the adsorption cell (which now contained the sample solution) was inserted into the front sample compartment. A Teflon tube connected to the tip of a thin N_2-bubling glass tube was lowered from one arm of the adsorption cell down the spectrophotometer cuvette to a level just above the light path to provide effective mixing. Finally, the carbon cloth, which had been removed temporarily after wetting and degassing, was re-inserted from the other arm of the adsorption cell into the solution. Then, quickly, an opaque curtain was spread above the sample compartment of the spectrophotometer, over the cell, to prevent interference from external light. A Cary 100 UV/VIS spectrophotometer was used for the optical absorbance measurements.

The scanning-kinetics program for monitoring the absorbance of the specific adsorbate was then run on the computer. This program enabled the absorbance spectrum to be recorded over a pre-selected, limited wavelength range in programmed time intervals (1 min). In this way, it was possible to record as many as about 1000 data points for an adsorption period of 1000 min at each wavelength in the selected region. This is one of the most important advantages of in-situ UV–visible spectroscopic technique as applied in scanning-kinetics mode. In most classical adsorption studies, batch analysis method is employed in which samples are withdrawn from the adsorption system at certain time intervals and analyzed ex-situ. Usually 10–20 data points could be obtained in such kinetic studies. Each sample withdrawal, of course, destructs the main adsorption system.

A typical scanning-kinetic output obtained during the adsorption of NaNS from water onto the ACC was reproduced in Fig. 2 in which only scans in 5 min intervals are shown. The downward movement of the absorbance maximum at 283 nm as the adsorption goes on is clearly seen in this figure and marked by an arrow. Any change in spectrum during the process could be seen in such a scanning-kinetic output. After completion of the adsorption run, a separate absorbance versus time curve could be printed at any wavelength in the scanned range. This wavelength is usually the one at one of the absorption maxima (λ_{max}) unless there is change in spectrum such as shift in λ_{max}.

Absorbance data were converted into concentration data using calibration relations pre-determined at the wavelength of maximum absorbance for each adsorbate. The calibration data for the benzene and naphthalene sulfonates studied are given in Table 2.

2.4. Determination of adsorption isotherms

The adsorption isotherms of adsorbates were determined on the basis of batch analysis. The ACC pieces of varying masses were allowed to equilibrate with solutions of adsorbates in water or in 0.01 M H_2SO_4 with known initial concentrations at 30 °C for 48 h. Preliminary tests showed that the concentration of adsorbates remained unchanged after 20–24 h contact with the ACC. So, the allowed contact time of 48 h ensures the equilibration. The equilibration was allowed in 100 mL Erlenmeyer flasks kept in Nüve ST 402 shaking waterbath at a constant shaking speed of 150 rpm. The concentrations after the equilibration period were measured spectrophotometrically. The amount of adsorbate adsorbed per unit mass of the ACC, q_e, was calculated by Eq. (1):

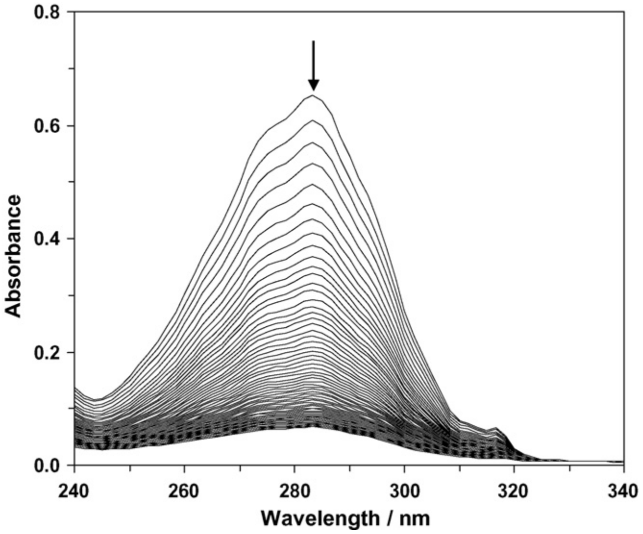

Fig. 2. Scans during the adsorption of NaNS onto the ACC in 5 min intervals over 300 min. Arrow shows direction of change (diminution) of optical absorbance maximum as the adsorption proceeds.

$$q_e = \frac{V(C_0 - C_e)}{m} \tag{1}$$

where V is the volume of the solution of adsorbate, C_0 and C_e are the initial and equilibrium concentrations, respectively, and m is the mass of the ACC.

3. Results and discussion

3.1. Adsorption kinetics

The concentration versus time plots for the adsorption of benzene and naphthalene sulfonates onto the ACC in water are shown in Fig. 3. It is seen that NaNS has the highest extent and rate of adsorption while Na_2BDS and Na_3NTS show similar and the lowest rate and extent of adsorption among other sulfonates. The removal percentages of the sulfonates studied at the end

Table 2
Spectral and calibration data for in-situ UV–visible spectroscopic analysis of benzene and naphthalene sulfonates. λ_{max}: wavelength of maximum absorption, ε: molar absorptivity, r: correlation coefficient.

Adsorbate	Solvent	λ_{max} (nm)	ε (M^{-1} cm^{-1})	r
NaBS	H_2O	212	7,800	0.9991
	0.01 M H_2SO_4	212	7,800	0.9994
Na_2BDS	H_2O	211	9,900	0.9995
	0.01 M H_2SO_4	211	10,000	0.9997
NaNS	H_2O	283	6,300	0.9999
	0.01 M H_2SO_4	283	6,300	0.9999
Na_2NDS	H_2O	287	9,600	0.9995
	0.01 M H_2SO_4	287	9,600	0.9999
Na_3NTS	H_2O	284	7,700	0.9999
	0.01 M H_2SO_4	284	7,700	0.9999

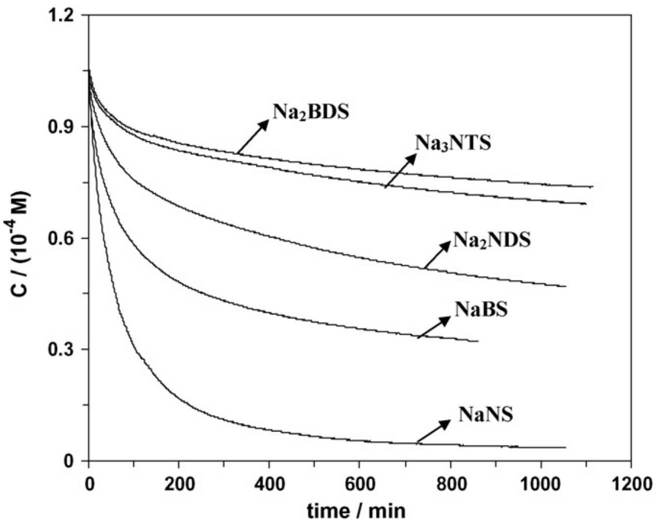

Fig. 3. Adsorption behaviors of benzene and naphthalene sulfonates from solutions in pure water. Initial concentration: 1×10^{-4} M, the amount of ACC: 18.3 ± 0.1 mg, the volume of adsorbate solution: 20 mL.

of 850 min of adsorption are increasing in the order Na_2BDS $\approx Na_3NTS < Na_2NDS <$ NaBS < NaNS having values of 28, 31, 50, 68 and 98%, respectively.

The initial pH values of all benzene and naphthalene sulfonate solutions are around 5.8 and increased only slightly at the end of the indicated adsorption periods. The pH values at the beginning and at the end of adsorption are listed in Table 3. Since these pH values are slightly lower than the $pH_{PZC} = 7.4$ of the ACC (Table 1), the net surface charge of the ACC is expected to be slightly positive [17]. Thus the ACC attracts the negatively charged sulfonate species by electrostatic interactions. However, considerable extents of adsorption of sulfonates from aqueous solutions observed in Fig. 3 may not only result from such marginal electrostatic interactions. Hydrophobic and π–π dispersion interactions are probably more important than the electrostatic interactions.

It can be seen that the above increasing order of extent of adsorption is also the increasing order of hydrophobic/hydrophilic ratio of the sulfonates studied. Number of sulfonate group per aromatic ring is 2, 3/2, 1, 1 and 1/2 for Na_2BDS, Na_3NTS, Na_2NDS, NaBS and NaNS, respectively, causing an increase in hydrophobicity in the same order.

It is clear from Fig. 3 that the adsorption extent and rate of NaNS is strikingly higher than all other sulfonates. This can be explained by the possible vertical orientation of NaNS at the surface of the ACC as proposed by O'Dea et al. [18]. After some theoretical calculations, these authors found interesting results for the adsorption of aromatic sulfonates onto graphite. They found that there is no bonding between sulfonates and graphite surface, molecules favor an arrangement with aromatic rings parallel to graphite surface and that the inclination of the aromatic sulfonates relative to graphite surface increases due to interactions between hydrophilic sulfonate groups and aqueous solutions. Furthermore, only naphthalene sulfonate, among other aromatic compounds and aromatic sulfonates, was found to favor a vertical orientation with the sulfonate group upwards when the solvent effects are included. This last conclusion of O'Dea et al. [18] based on theoretical calculations is in good agreement with our experimental finding that the rate and extent of adsorption of NaNS is by far higher than those of other sulfonates. Vertical orientation of NaNS leads to faster adsorption due to less lateral interactions between them at the surface and to higher extent of adsorption due to smaller area occupation at the surface.

Table 3
The pH values of adsorbate solutions in H_2O at the beginning (pH_i) and at the end of adsorption (pH_f) during isotherm studies.

Adsorbate	Solvent	pH_i	pH_f[a]
NaBS	H_2O	5.78	5.91–6.18
	0.01 M H_2SO_4	1.98	2.00–2.05
Na_2BDS	H_2O	5.83	5.99–6.15
	0.01 M H_2SO_4	1.99	2.00–2.07
NaNS	H_2O	5.81	5.95–6.31
	0.01 M H_2SO_4	1.96	1.99–2.06
Na_2NDS	H_2O	5.87	5.90–6.25
	0.01 M H_2SO_4	1.97	1.99–2.07
Na_3NTS	H_2O	5.80	5.84–6.17
	0.01 M H_2SO_4	1.98	2.00–2.08

[a] pH_f values varied with the amount of the ACC used in isotherm studies. Thus a range is given for this value.

It is known that the sulfonate group is an electron withdrawing group and thus the electron densities on aromatic rings of sulfonates increase in the same order as their extents of adsorption. For this reason, it can be said that if the electron density of aromatic ring of the adsorbate increases, adsorption extent of adsorbate onto the adsorbent also increases. Therefore the π–π dispersion interactions seem to be extremely important in determining the extent of adsorption of aromatic sulfonates.

Another important factor in determining the extent of adsorption is the size of adsorbate species. The widths and lengths of benzene and naphthalene sulfonates were determined using a program called ChemSketch. The dimensions (widths × lengths) of NaBS, Na_2BDS, NaNS, Na_2NDS and Na_3NTS are found to be (4.8 × 7.0), (7.0 × 7.0), (7.0 × 7.6) (7.0 × 10.8) and (8.8 × 8.8) Å, respectively. On the other hand, the percentage of total pores of the ACC having pore size greater than 4.8, 7.0, 7.6, 8.8 and 10.8 Å were 98, 80, 78, 67 and 52, respectively, as deduced from the pore size distribution curve given in our earlier works [6,13]. It is seen that more than 78% of the total pores are available for NaBS, Na_2BDS and NaNS. It is also seen that smaller percentages of pores available for the adsorption of Na_2NDS and Na_3NTS have important contribution, beside their higher hydrophilicity, for their smaller rates and extents of adsorption.

Adsorption experiments were repeated in 0.01 M H_2SO_4 solutions in order to investigate the effect of electrostatic interactions. Since pH_{PZC} of the ACC is 7.4 (Table 1), the surface will acquire high positive charge at low pH values in 0.01 M H_2SO_4 [17]. Initial and final pH values for adsorption from 0.01 M H_2SO_4 are recorded in Table 3. Sulfonic acids, being strong acids, will still be mainly in negatively charged sulfonate state in 0.01 M H_2SO_4. For example, the K_a value of benzene sulfonic acid is 0.7 [19]. The analytical calculation using this K_a value shows that the anion of NaBS maintains its anionic form in 0.01 M H_2SO_4 solutions. So, the adsorption of sulfonates is expected to be enhanced in acidic solutions compared to solutions in pure water due to stronger electrostatic attractions in acidic solutions. The adsorption behaviors of benzene and naphthalene sulfonates from 0.01 M H_2SO_4 solutions are shown in Fig. 4. It is clearly seen by visual comparison of adsorption curves in Fig. 3 with the corresponding curves in Fig. 4 that the rates and extends of adsorption of sulfonates are greatly enhanced in 0.01 M H_2SO_4 solution. The primary reason for this enhancement is expected to be the increased electrostatic attraction between highly positive charged ACC and the negatively charged sulfonate anions. The removal percentages of NaBS, Na_2BDS, NaNS, Na_2NDS and Na_3NTS in 0.01 M H_2SO_4 solutions after 1200 min are 98, 99, 100, 100 and 99, respectively, indicating almost complete removal.

In order to make more quantitative kinetic evaluation and to investigate the adsorption mechanism of benzene and naphthalene

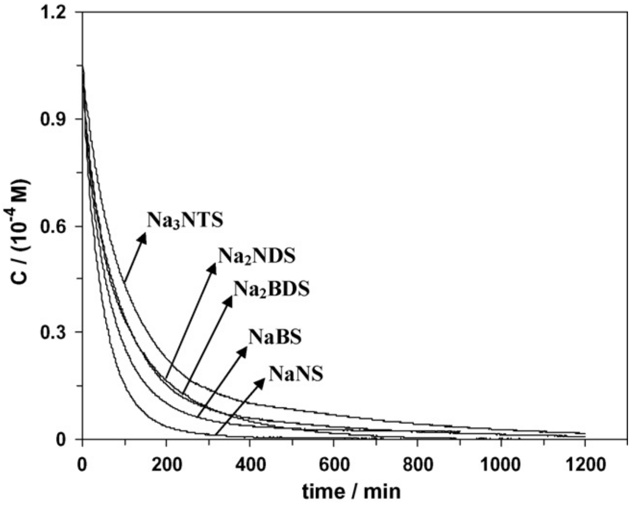

Fig. 4. Adsorption behaviors of benzene and naphthalene sulfonates from 0.01 M H_2SO_4 solutions. Initial concentration: 1×10^{-4} M, the amount of ACC: 18.3 ± 0.1 mg, the volume of adsorbate solution: 20 mL.

sulfonates onto the ACC, the kinetic data presented in Figs. 3 and 4 were tested according to some well-known kinetic models, such as pseudo first-order, pseudo second-order, Elovich and intra-particle diffusion. The mathematical expressions for the pseudo first-order rate equation of Lagergren [20], the pseudo second-order rate equation [21–23] and Elovich equation [21,24] are given in Eqs. (2), (3) and (4), respectively:

$$\ln(q_e - q_t) = \ln q_e - k_1 t \tag{2}$$

$$\frac{t}{q_t} = \frac{1}{k_2 q_e^2} + \frac{1}{q_e} t \tag{3}$$

$$q_t = \beta \ln(\alpha\beta) + \beta \ln t \tag{4}$$

In these equations q_e is the amount of sulfonate adsorbed per unit mass of the ACC at equilibrium, q_t is that at time t, k_1 is the first-order rate constant, k_2 is the second-order rate constant, α and β are Elovich coefficients. All kinetic equations (Eqs. (2), (3) and (4)) are in linear form and the parameters of them can be determined from linear regression analysis of the experimental kinetic data; $\ln(q_e - q_t)$ versus t in Eq. (2), t/q_t versus t in Eq. (3) and q_t versus $\ln t$ in Eq. (4). It is convenient to define the product $k^2 q_e^2$ in Eq. (3) as the initial sorption rate and denote by h. All these parameters and regression coefficients for treatment according to each kinetic equation are given in Table 4.

Regression coefficient values of pseudo second-order model for adsorption of benzene and naphthalene sulfonates onto the ACC ($r > 0.994$) are higher than those of pseudo first-order and Elovich models. This suggests that the adsorption of benzene and naphthalene sulfonates under study follows the pseudo second-order kinetic model.

Pseudo second-order rate constants of benzene and naphthalene sulfonates decreased in the order of $NaNS > NaBSA \approx Na_2BDS > Na_3NTS > Na_2NDS$ in water solutions and $NaNS > NaBS > Na_2BDS > Na_2NDS > Na_3NTS$ in 0.01 M H_2SO_4 solutions (Table 4). On the other hand initial sorption rate values (h) of benzene and naphthalene sulfonates increased in the order of $Na_3NTS \approx Na_2BDS < Na_2NDS < NaBS < NaNS$ in water solutions and $Na_3NTS < Na_2BDS \approx Na_2NDS < NaBS < NaNS$ in 0.01 M H_2SO_4 solutions (Table 4). This final order according to h values is in agreement with the visually observed adsorption behavior in Figs. 3 and 4.

Adsorption proceeds in several steps involving transport of the solute molecules from the aqueous phase to the surface of the adsorbent and then their diffusion into the interior of the pores. The latter step is usually a slow process. The intra-particle diffusion rate constant, k_i, is given by the following equation [25]:

$$q_t = k_i t^{0.5} \tag{5}$$

When intra-particle diffusion plays a significant role in controlling the kinetics of the adsorption process, the plots of q_t versus $t^{0.5}$ yield straight lines passing through the origin and the slope gives the rate constant, k_i. The plots of q_t versus $t^{0.5}$ for the present results did not yield a straight line passing through the origin. This suggested that the intra-particle diffusion model is not the rate-limiting control step for the adsorption of benzene and naphthalene sulfonates.

3.2. Adsorption isotherms

Adsorption isotherm data obtained at 30 °C in water and in 0.01 M H_2SO_4 are given in Fig. 5 for NaBS and Na_2BDS, and in Fig. 6 for NaNS, Na_2NDS and Na_3NTS. The isotherm data were treated according to two well-known isotherm equations; Langmuir and Freundlich. The linearized forms of Langmuir and Freundlich isotherm equations can be given in Eqs. (6) and (7), respectively [26]:

$$\frac{C_e}{q_e} = \frac{C_e}{q_{\max}} + \frac{1}{b q_{\max}} \tag{6}$$

$$\ln q_e = \ln K_F + \frac{1}{n} \ln C_e \tag{7}$$

where q_e is the amount of adsorbate adsorbed per unit mass of adsorbent at equilibrium, C_e is the final concentration at equilibrium, q_{max} is the maximum adsorption at monolayer coverage, b

Table 4
The parameters and regression coefficients of the three kinetic models applied for experimental adsorption kinetic data of the benzene and naphthalene sulfonates.

Adsorbate	Solvent	Pseudo first-order		Pseudo second-order			Elovich equation		
		$k_1 \times 10^3$ (min^{-1})	r	k_2 (mmol (g min)$^{-1}$)	$h \times 10^3$ (g (mmol min)$^{-1}$)	r	α (g (mmol min)$^{-1}$)	$\beta \times 10^3$ (mmol (g min)$^{-1}$)	r
NaBS	H_2O	5.01	0.9542	0.164	1.10	0.9996	24.3	13.8	0.9950
	0.01 M H_2SO_4	7.30	0.9857	0.276	3.59	0.9996	52.2	17.5	0.9344
Na_2BDS	H_2O	3.30	0.9584	0.176	0.254	0.9961	24.3	6.50	0.9917
	0.01 M H_2SO_4	4.80	0.9803	0.189	2.60	0.9999	43.8	17.6	0.9454
NaNS	H_2O	5.40	0.9877	0.213	2.80	0.9999	59.6	16.7	0.9566
	0.01 M H_2SO_4	5.40	0.9070	0.554	7.57	0.9998	444	14.0	0.8691
Na_2NDS	H_2O	3.70	0.9478	0.0941	0.438	0.9965	10.5	12.2	0.9898
	0.01 M H_2SO_4	6.80	0.9835	0.162	2.42	0.9997	27.9	14.2	0.8709
Na_3NTS	H_2O	3.40	0.9450	0.131	0.238	0.9938	15.6	7.50	0.9831
	0.01 M H_2SO_4	4.40	0.9614	0.113	1.56	0.9997	14.3	20.0	0.9648

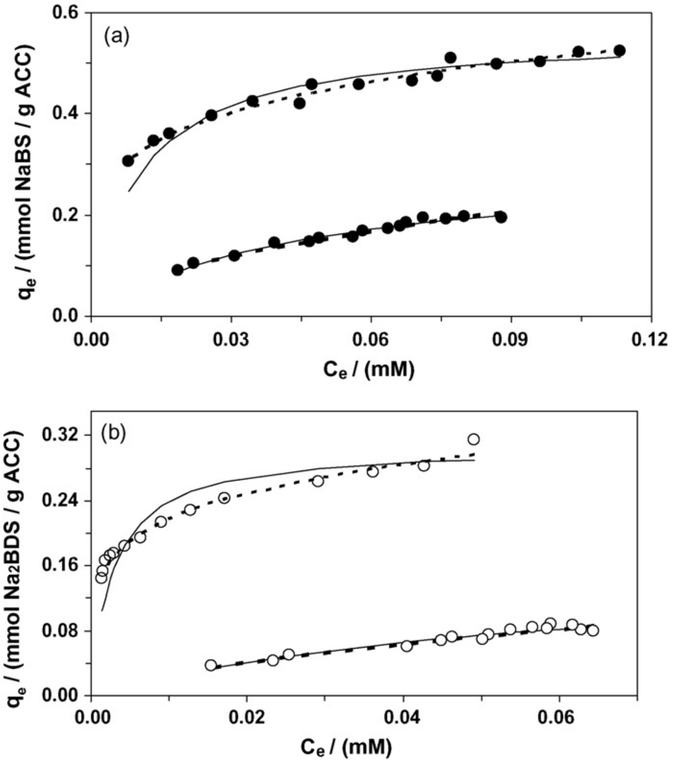

Fig. 5. Adsorption isotherms of (a) NaBS and (b) Na_2BDS from solutions in water (lower curves and data in each figure) and from 0.01 M H_2SO_4 solutions (upper curves and data in each figure). (—) Langmuir isotherm and (. . .) Freundlich isotherm.

is the adsorption equilibrium constant related to the energy of adsorption, K_F is the Freundlich constant representing the adsorption capacity and n is a constant related to surface heterogeneity. Freundlich constant, $1/n$, is also a measure of the deviation of the adsorption from linearity. If $1/n$ is equal to unity the adsorption isotherm becomes linear. This means that the adsorption sites are homogeneous in energy and no interaction take place between the adsorbed species. If the value of $1/n$ is smaller than 1, adsorption is favorable. When the value of $1/n$ is larger than 1, the adsorption interactions become weak and unfavorable adsorption takes place [27].

The parameters of Eqs. (6) and (7) were obtained by linear regression analysis of experimental isotherm data. The obtained parameters are given in Table 5. The regression coefficients are higher than 0.92 for both isotherm models and for all sulfonates.

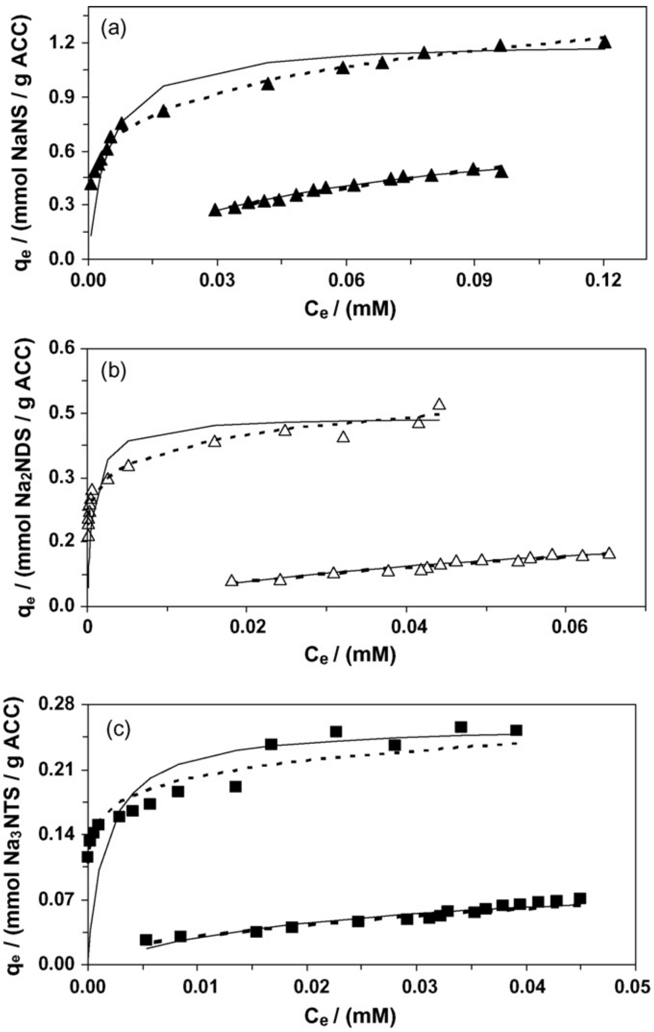

Fig. 6. Adsorption isotherms of (a) NaNS, (b) Na_2NDS and (c) Na_3NTS from solutions in water (lower curves and data in each figure) and from 0.01 M H_2SO_4 solutions (upper curves and data in each figure). (—) Langmuir isotherm and (. . .) Freundlich isotherm.

Thus it is difficult to judge which isotherm model is best for representing the experimental isotherm data. A better criterion for the assessment of experimental isotherm data is a parameter known as normalized percent deviation [28] or in some literature as percent relative deviation modulus, P [29,30], given by the following

Table 5
Parameters of Langmuir and Freundlich isotherm equations, regression coefficients (r) and normalized percent deviation (P) values for benzene and naphthalene sulfonates at 30 °C.

Adsorbate	Solvent	Langmuir parameters				Freundlich parameters			
		q_{max} (mmol g^{-1})	b (L $mmol^{-1}$)	r	P	K_F (mmol g^{-1}) (L $mmol^{-1}$)$^{1/n}$	$1/n$	r	P
NaBS	H_2O	0.301	22.2	0.9878	2.78	0.716	0.512	0.9901	2.57
	0.01 M H_2SO_4	0.558	97.5	0.9971	4.21	0.813	0.200	0.9898	1.73
Na_2BDS	H_2O	0.167	16.1	0.9261	4.96	0.484	0.629	0.9817	4.57
	0.01 M H_2SO_4	0.307	350	0.9952	11.9	0.528	0.192	0.9924	2.20
NaNS	H_2O	0.834	15.9	0.9917	1.78	1.82	0.538	0.9918	2.02
	0.01 M H_2SO_4	1.21	217	0.9973	15.1	1.89	0.203	0.9963	2.29
Na_2NDS	H_2O	0.246	15.2	0.9274	4.31	0.667	0.615	0.9799	3.88
	0.01 M H_2SO_4	0.441	1333	0.9961	29.6	0.687	0.138	0.9857	3.91
Na_3NTS	H_2O	0.100	40.2	0.9242	8.85	0.291	0.484	0.9727	6.35
	0.01 M H_2SO_4	0.258	616	0.9947	24.4	0.347	0.117	0.9444	7.40

equation:

$$P = \frac{100}{N}\sum_{i=1}^{N}\frac{\left|q_{e(pred)} - q_{e(\exp)}\right|}{q_{e(\exp)}} \quad (8)$$

where $q_{e(exp)}$ is the experimental q_e at any C_e, $q_{e(pred)}$ is the corresponding q_e predicted from the equation under study with the best fitted parameters and N is the number of observations. It is clear that the smaller the P value, the better is the fit. It is generally accepted that when the P value is less than 5, the fit is considered to be excellent [29]. The P values for Freundlich model are generally found to be smaller than those for Langmuir model (Table 5). Thus, it can be concluded that Freundlich isotherm model represents the experimental isotherm data better than Langmuir model for the benzene and naphthalene sulfonates under study. Freundlich constant, K_F, representing the adsorption capacity (Table 5) increased in the order $Na_3NTS < Na_2BDS \approx Na_2NDS < NaBS < NaNS$ in water and in 0.01 M H_2SO_4 solutions. This result is in agreement with that found on the basis of kinetic data in the previous section. The values of $1/n$ are found to be less than 1 (Table 5), suggesting favorable adsorption behavior of benzene and naphthalene sulfonates onto the ACC.

4. Conclusions

The highest extent and rate of adsorption observed for NaNS among the five sulfonates studied were found to be due to vertical orientation of NaNS at the ACC surface as supported by the results of some theoretical calculations of O'Dea et al. [18]. The order of rate and extent of adsorption for the sulfonates was in agreement with the order of degree of hydrophobocity of sulfonates. Kinetic data for the adsorption of sulfonates from solutions in water and in 0.01 M H_2SO_4 were well fitted to pseudo second-order equation. The isotherm data were found to be better represented by Freundlich model than Langmuir model. Further experiments are being designed to improve the extent of adsorption of adsorbates onto the ACC in the future works. One of such promising methods is electro-assisted adsorption known as electrosorption. Another experiment to design might be the adsorption from adsorbate solutions containing other species together with the target adsorbate, such as salts, to simulate the real waste-water systems.

Acknowledgements

The authors would like to thank to the Scientific Research Projects Unit of Akdeniz University for the support of this work through the project 2003.03.0121.012.

References

[1] M.C. Alonso, D. Barcelo, Stability study and determination of benzene and naphthalenesulfonates following an on-line solid-phase extraction method using the new programmable field extraction system, Analyst 127 (2002) 472–479.

[2] M. Howe-Grant, Kirk-Othmer Encyclopedia of Chemical Technology, John-Wiley & Sons, New York, 1992.

[3] S. Ruckstuhl, M.J.F. Suter, W. Giger, Rapid determination of sulfonated naphthalenes and their formaldehyde condensates in aqueous environmental samples using synchronous excitation fluorimetry, Analyst 126 (2001) 2072–2077.

[4] A. Sakoda, M. Suzuki, R. Hirai, K. Kawazoe, Trihalomethane adsorption on activated carbon fibers, Water Res. 25 (1991) 219–225.

[5] H. Grajek, S. Neffe, Z. Witkiewicz, Chromatographic determination of the physicochemical parameters of adsorption on activated carbon fibres, J. Chromatogr. A 600 (1992) 67–77.

[6] O. Duman, E. Ayranci, Adsorption characteristics of benzaldehyde, sulphanilic acid and p-phenolsulfonate from water, acid or base solutions onto activated carbon cloth, Sep. Sci. Technol. 41 (2006) 3673–3692.

[7] C. Sheindorf, M. Rebhun, M. Sheintuch, Organic pollutants adsorption from multicomponent systems modeled by Freundlich type isotherm, Water Res. 16 (1982) 357–362.

[8] J. Rivera-Utrilla, M. Sanchez-Polo, F. Carrasco-Marin, Adsorption of 1,3,6-naphthalenetrisulfonic acid on activated carbon in the presence of Cd(II), Cr(III) and Hg(II). Importance of electrostatic interactions, Langmuir 19 (2003) 10857–10861.

[9] A. Esposito, A. Del Borghi, F. Veglio, Investigation of naphthalene sulfonate compounds sorption in a soil artificially contaminated using batch and column assays, Waste Manage. 22 (2002) 937–943.

[10] E. Ayranci, B.E. Conway, Removal of phenol, phenoxide and chlorophenols from waste-waters by adsorption and electrosorption at high-area carbon felt electrodes, J. Electroanal. Chem. 513 (2001) 100–110.

[11] O. Duman, E. Ayranci, Structural and ionization effects on the adsorption behaviors of some anilinic compounds from aqueous solution onto high-area carbon cloth, J. Hazard. Mater. 120 (2005) 173–181.

[12] E. Ayranci, O. Duman, Adsorption behaviors of some phenolic compounds onto high specific area activated carbon cloth, J. Hazard. Mater. 124 (2005) 125–132.

[13] E. Ayranci, O. Duman, Adsorption of aromatic organic acids onto high area activated carbon cloth in relation to wastewater purification, J. Hazard. Mater. 136 (2006) 542–552.

[14] E. Ayranci, B.E. Conway, Adsorption and electrosorption of ethyl xanthate and thiocyanate anions at high-area carbon-cloth electrodes studied by in-situ UV spectroscopy: development of procedures for wastewater purification, Anal. Chem. 73 (2001) 1181–1189.

[15] E. Ayranci, B.E. Conway, Adsorption and electrosorption at high-area carbon felt electrodes for waste-water purification systems evaluation with inorganic, S-containing anion, J. Appl. Electrochem. 31 (2001) 257–266.

[16] B.E. Conway, G. Ayranci, E. Ayranci, Molecular structure effects in the adsorption behavior of some aromatic heterocyclic compounds at high-area carbon cloth in relation to waste-water purification, Z. Phys. Chem. 217 (2003) 315–331.

[17] C. Moreno-Castilla, Adsorption of organic molecules from aqueous solutions on carbon materials, Carbon 42 (2004) 83–94.

[18] A.R. O'Dea, R.St.C. Smart, A.R. Gerson, Molecular modeling of the adsorption of aromatic and aromatic sulfonate molecules from aqueous solutions onto graphite, Carbon 37 (1999) 1133–1142.

[19] A.E. Martell, R.M. Smith, Critical Stability Constants, Plenum Press, New York, 1989.

[20] S. Lagergren, About the Theory of so-called Adsorption of Soluble Substances, 24, Kungliga Svenska Vetenskapsakademiens, Handlingar, 1898, pp. 1–39.

[21] G. McKay, Y.S. Ho, J.C.Y. Ng, Biosorption of copper from waste waters: a review, Sep. Purif. Methods 28 (1999) 87–125.

[22] S. Azizian, A novel and simple method for finding the heterogeneity of adsorbents on the basis of adsorption kinetic data, J. Colloid Interface Sci. 302 (2006) 76–81.

[23] S. Azizian, kinetic models of sorption: a theoretical analysis, J. Colloid Interface Sci. 276 (2004) 47–52.

[24] S.H. Chien, W.R. Clayton, Application of Elovich equation to the kinetics of phosphate release and sorption in soils, Soil Sci. Soc. Am. J. 44 (1980) 265–268.

[25] W.J. Weber, J.C. Morris, Kinetics of adsorption on carbon solution, J. Sanit. Eng. Div. Am. Soc. Civil Eng. 89 (1963) 31–59.

[26] J.M. Smith, Chemical Engineering Kinetics, McGraw-Hill Company, New York, 1981.

[27] A.S. Ozcan, B. Erdem, A. Ozcan, Adsorption of acid blue 193 from aqueous solutions onto Na-bentonite and DTMA-bentonite, J. Colloid Interface Sci. 280 (2004) 44–54.

[28] R.S. Juang, R.L. Tseng, F.C. Wu, S.H. Lee, Liquid-phase adsorption of phenol and its derivatives on activated carbon fibers, Sep. Sci. Technol. 31 (1996) 1915–1931.

[29] C.J. Lomauro, A.S. Bakshi, T.P. Labuza, Evaluation of food moisture sorption isotherm equations. Part I. Fruit, vegetable and meat products, Lebensm. Wiss. Technol. 18 (1985) 111–117.

[30] E. Ayranci, O. Duman, Moisture sorption isotherms of cowpea (Vigna unguiculata L. Walp) and its protein isolate at 10, 20 and 30 °C, J. Food Eng. 70 (2005) 83–91.